NASA TECHNICAL MEMORANDUM

NASA TM X-2021

LOW-SPEED STATIC STABILITY AND CONTROL CHARACTERISTICS OF TWO SMALL-SCALE, HYPERSONIC CRUISE CONFIGURATIONS

by Delma C. Freeman, Jr., and Richard S. Jones

Langley Research Center
Hampton, Va. 23365

1. Report No. NASA TM X-2021	2. Government Accession No.	3. Recipient's Catalog No.
4. Title and Subtitle LOW-SPEED STATIC STABILITY AND CONTROL CHARAC-TERISTICS OF TWO SMALL-SCALE, HYPERSONIC CRUISE CONFIGURATIONS		5. Report Date June 1970
		6. Performing Organization Code
7. Author(s) Delma C. Freeman, Jr., and Richard S. Jones		8. Performing Organization Report No. L-7134
9. Performing Organization Name and Address NASA Langley Research Center Hampton, Va. 23365		10. Work Unit No. 722-01-10-07
		11. Contract or Grant No.
12. Sponsoring Agency Name and Address National Aeronautics and Space Administration Washington, D.C. 20546		13. Type of Report and Period Covered Technical Memorandum
		14. Sponsoring Agency Code

15. Supplementary Notes

16. Abstract

   A wind-tunnel investigation has been conducted to determine the low-speed static stability and control characteristics of two small-scale, hypersonic cruise configurations — a distinct wing-body configuration and a blended wing-body configuration.

17. Key Words (Suggested by Author(s)) Hypersonic cruise vehicle Delta-wing configuration		18. Distribution Statement Unclassified — Unlimited		
19. Security Classif. (of this report) Unclassified	20. Security Classif. (of this page) Unclassified		21. No. of Pages 25	22. Price* $3.00

LOW-SPEED STATIC STABILITY AND CONTROL CHARACTERISTICS OF
TWO SMALL-SCALE, HYPERSONIC CRUISE CONFIGURATIONS

By Delma C. Freeman, Jr., and Richard S. Jones
Langley Research Center

SUMMARY

A wind-tunnel investigation has been conducted to determine the low-speed static stability and control characteristics of two small-scale, hypersonic cruise configurations − a distinct wing-body configuration and a blended wing-body configuration.

The investigation showed that the distinct wing-body configuration with its center of gravity located at 0.51 of the mean aerodynamic chord (landing configuration) was statically longitudinally unstable up to the stall and directionally unstable at angles of attack above about 8°. The blended wing-body configuration with its center of gravity located at 0.37 of the mean aerodynamic chord was statically longitudinally unstable over most of the test angle-of-attack range and directionally stable up to the stall.

INTRODUCTION

For the past few years the National Aeronautics and Space Administration has been conducting studies directed toward providing information to help in the development of a hypersonic cruise vehicle. From the results of preliminary studies accounting for the interplay between structures, propulsion, and aerodynamics (refs. 1 and 2), two hypersonic cruise configurations have evolved. The Langley Research Center has conducted wind-tunnel tests to evaluate the aerodynamic characteristics of these configurations throughout the Mach number range. (See refs. 1 and 3.) As part of this general effort, the present wind-tunnel investigation has consisted of static force tests to determine the low-speed longitudinal and lateral stability and control characteristics of two configurations: a delta-wing vehicle with a distinct body, wing, and horizontal tail and a blended wing-body vehicle with a double-delta planform and elevons for control.

SYMBOLS

The longitudinal data are referred to the stability system of axes and the lateral data are referred to the body system of axes. (See fig. 1.) The origins of the axes were located to correspond to the center-of-gravity positions presented in figure 2. These

center-of-gravity positions (0.51 of the mean aerodynamic chord for the distinct wing-body configuration and 0.37 of the mean aerodynamic chord for the blended wing-body configuration) were specified in the preliminary study (ref. 2) for the landing configuration.

In order to facilitate international usage of data presented, dimensional quantities are presented in both the U.S. Customary Units and the International System of Units (SI). The equivalent dimensions were determined in each case by using the conversion factors give in reference 4.

b wing span, ft (m)

C_L lift coefficient, F_L/qS

C_l rolling-moment coefficient, M_X/qSb

ΔC_l incremental rolling-moment coefficient

$C_{l\beta} = \dfrac{\partial C_l}{\partial \beta}$, per deg

C_m pitching-moment coefficient, $M_Y/qS\bar{c}$

C_n yawing-moment coefficient, M_Z/qSb

ΔC_n incremental yawing-moment coefficient

$C_{n\beta} = \dfrac{\partial C_n}{\partial \beta}$, per deg

C_Y side-force coefficient, F_Y/qS

ΔC_Y incremental side-force coefficient

$C_{Y\beta} = \dfrac{\partial C_Y}{\partial \beta}$, per deg

$\bar{c}$ mean aerodynamic chord, ft (m)

F_D drag force, lb (N)

F_L lift force, lb (N)

F_Y lateral force, lb (N)

2

i_t	horizontal-tail incidence, positive when trailing edge is down, deg
M_X	rolling moment, ft-lb (N-m)
M_Y	pitching moment, ft-lb (N-m)
M_Z	yawing moment, ft-lb (N-m)
q	dynamic pressure, lb/ft^2 (N/m^2)
S	wing area, ft^2 (m^2)
X,Y,Z	body reference axes
X_s,Y_s,Z_s	stability reference axes
α	angle of attack, deg
β	angle of sideslip, deg
δ_a	total aileron deflection, $\delta_{e,L} - \delta_{e,R}$, deg
δ_e	elevon deflection, positive when trailing edge is down, deg
$\delta_{e,L}$	left elevon deflection, positive when trailing edge is down, deg
$\delta_{e,R}$	right elevon deflection, positive when trailing edge is down, deg
$\delta_{i,t}$	differential deflection of horizontal tail used for roll control, positive when trailing edge of right surface is down, deg
δ_r	rudder deflection, positive when trailing edge is deflected to left, deg
ψ	angle of yaw, deg

APPARATUS AND MODEL.

Drawings of the models used in this investigation are presented in figure 2. The distinct wing-body configuration, presented in figure 2(a), consisted of a 65° swept wing of delta planform, horizontal and vertical tails, and a flow-through engine nacelle under

the fuselage. The model had a conventional rudder for directional control and utilized differential deflection of the all-movable horizontal tail for roll control. The blended wing-body configuration presented in figure 2(c) had a double-delta planform with 65° sweep on the rear delta, a flow-through engine nacelle under the fuselage, and elevon surfaces for both roll and pitch control. Photographs of the models are presented in figure 3.

The static force tests were conducted in a low-speed tunnel with a 12-ft (3.6-m) octagonal test section at the Langley Research Center.

TESTS

Force tests were made to determine the static longitudinal and lateral stability and control characteristics of the two configurations. The tests were generally made over an angle-of-attack range from -4° to 30°. The lateral-force and moment data were measured over a sideslip-angle range at fixed angles of attack. The lateral stability derivatives were determined from the incremental differences in C_n, C_l, and C_Y measured at $\pm 5^\circ$ sideslip. The force tests were made at a velocity of 72.2 ft/sec (22 m/sec), which corresponds to a Reynolds number per foot of 0.46×10^6 (per meter, 1.51×10^6).

RESULTS AND DISCUSSION

Static Longitudinal Characteristics

Distinct wing-body configuration.- The static longitudinal characteristics of the distinct wing-body configuration are presented in figure 4 for the center-of-gravity position for the landing configuration ($0.51\bar{c}$). The data show that the configuration with this center of gravity was longitudinally unstable up to about the stall ($\alpha \approx 25^\circ$). These data also show that the horizontal tail was effective for providing pitch control.

Data presented in figure 5 show the effect on the static longitudinal characteristics of moving the reference center of gravity to a location representative of the cruise configuration ($0.37\bar{c}$). Even with the forward center of gravity the model was unstable at an angle of attack from about 5° to 15° and the pitching moment was very nonlinear.

In an effort to establish the reason for the longitudinal instability, tests were made to determine the contribution of various components to the stability of the model. Resulting data presented in figure 6 show that the model had about the same degree of instability with the horizontal tail off or on and thereby indicate that the tail was ineffective as a stabilizer. Data for horizontal tail on and wing off showed expected effectiveness of the tail. From these results it appears that the tail is in the wing downwash field, and as a result there is a loss of effectiveness. This conclusion was supported by some smoke-flow studies which showed the vortex flow from the delta wing acting on the tail.

4

Because the ineffectiveness of the horizontal tail was apparently caused by the position of the tail relative to the wing, additional tests were made to study the effect of varying the vertical position of the horizontal tail. (See fig. 2(b).) Resulting data presented in figure 7 show that a configuration with either a midtail or a T-tail arrangement was stable in the low angle-of-attack range. The configuration became unstable, however, as the angle of attack increased and the tail again moved into the wing downwash field.

Blended wing-body configuration.- Presented in figure 8 are the static longitudinal stability and control characteristics of the blended wing-body configuration. The data show that the configuration with the landing center of gravity ($0.37\bar{c}$) was statically unstable over the test angle-of-attack range except near 0°. Instability at low speeds is not generally characteristic of delta wings and is apparently associated with the lift of the forward delta of the wing which moves the aerodynamic center forward. This result has been noted in previous tests of similar configurations, for example, the double-delta supersonic transport configuration presented in reference 5. The data of figure 8 also show that the elevon effectiveness for pitch control was about constant at angles of attack up to 20°.

<center>Static Lateral Characteristics</center>

Distinct wing-body configuration.- The variations of the static lateral characteristics with angle of sideslip for the distinct wing-body configuration at several angles of attack are presented in figure 9. The data indicate a generally linear variation of the coefficients over the sideslip range of the test ($-10^{\circ} \le \beta \le 10^{\circ}$).

The variations of the lateral derivatives with angle of attack are presented in figure 10 for the complete configuration and for the configuration with various components removed. The data show that the complete configuration is directionally unstable at an angle of attack above about 8° and has negative effective dihedral $\left(+C_{l_\beta}\right)$ at an angle of attack near 15°. The instability is caused by the large destabilizing moment of the wing-body combination which overpowers the stabilizing effect of the vertical tail. It is interesting to note that the wing contributes a large positive increment of directional stability at an angle of attack up to about 10°.

The variation of the roll control effectiveness of the differentially deflected horizontal tail with angle of attack for the distinct wing-body configuration is presented in figure 11. The data show that the rolling moment produced by the horizontal tail was essentially constant through the stall. Large proverse yawing moments were also produced, however, and the yawing moments were up to twice as large as the rolling moments, depending on the amount of tail deflection. The large proverse yawing moments are typical of this type of roll control for which the differentially deflected surfaces are close to a center vertical tail and result in a pressure differential across the vertical tail.

Presented in figure 12 is the variation of the rudder control effectiveness with angle of attack for the distinct wing-body configuration. The data show that rudder control effectiveness was maintained over the test angle-of-attack range and that rudder deflection produced small adverse rolling moments.

Blended wing-body configuration.- The variations of the lateral characteristics with angle of sideslip for the blended wing-body configuration at several angles of attack are presented in figure 13. The data show a generally linear variation of the coefficients over the sideslip range ($-10^O \leq \beta \leq 10^O$) at an angle of attack up to 15°. At higher angles of attack the curves not only became nonlinear but also changed slope.

The variations of the static lateral stability derivatives with angle of attack are presented in figure 14. The data show that the blended wing-body configuration is directionally stable up to about the stall ($\alpha \approx 23^O$) although the stability decreases rather rapidly at an angle of attack above 15°. The configuration has positive effective dihedral $\left(-C_{l_\beta}\right)$ over the test angle-of-attack range, and the effective dihedral also decreases at angles of attack above 15°.

The variation of the aileron effectiveness with angle of attack is presented in figure 15. The data show that roll control effectiveness is maintained over the test angle-of-attack range and there are generally proverse yawing moments generated. The ratio of the yawing moment to rolling moment is much smaller than that for the distinct wing-body configuration.

The variation of the rudder control effectiveness with angle of attack is presented in figure 16. The data show that the rudder effectiveness is maintained at a relatively constant level over the angle-of-attack range. Some adverse rolling moment is generated by rudder deflection.

<div align="center">SUMMARY OF RESULTS</div>

The results of an investigation to determine the low-speed static stability and control characteristics of two small-scale, hypersonic cruise configurations may be summarized as follows:

1. The distinct wing-body configuration with its center of gravity located at 0.51 of the mean aerodynamic chord was statically longitudinally unstable up to about the stall.

2. The blended wing-body configuration with its center of gravity located at 0.37 of the mean aerodynamic chord had neutral static longitudinal stability near zero angle of attack; however, the configuration became increasingly unstable as the angle of attack increased.

3. The distinct wing-body and the blended wing-body configurations became directionally unstable at angles of attack of about 8° and 23°, respectively.

4. Both configurations had roll control effectiveness over the test angle-of-attack range. The roll control of the distinct wing-body configuration, however, produced proverse yawing moments that were larger than the rolling moments.

Langley Research Center,
    National Aeronautics and Space Administration,
        Hampton, Va., March 8, 1970.

REFERENCES

1. Penland, Jim A.; Edwards, Clyde L. W.; Witcofski, Robert D.; and Marcum, Don C., Jr.: Comparative Aerodynamic Study of Two Hypersonic Cruise Aircraft Configurations Derived From Trade-Off Studies. NASA TM X-1436, 1967.

2. Jarlett, F. E.: Performance Potential of Hydrogen Fueled, Airbreathing Cruise Aircraft. Vols. 1-4, Rep. No. GD/C-DCB66-004/1-4 (Contract NAS 2-3180), Gen. Dyn., Sept. 30, 1966.

3. Langhans, Richard A.: Transonic Aerodynamic Characteristics of Two Hypersonic Cruise Configurations. NASA TM X-1816, 1969.

4. Mechtly, E. A.: The International System of Units — Physical Constants and Conversion Factors. NASA SP-7012, 1964.

5. Freeman, Delma C., Jr.: Low-Subsonic Flight and Force Investigation of a Supersonic Transport Model With a Double-Delta Wing. NASA TN D-4179, 1968.
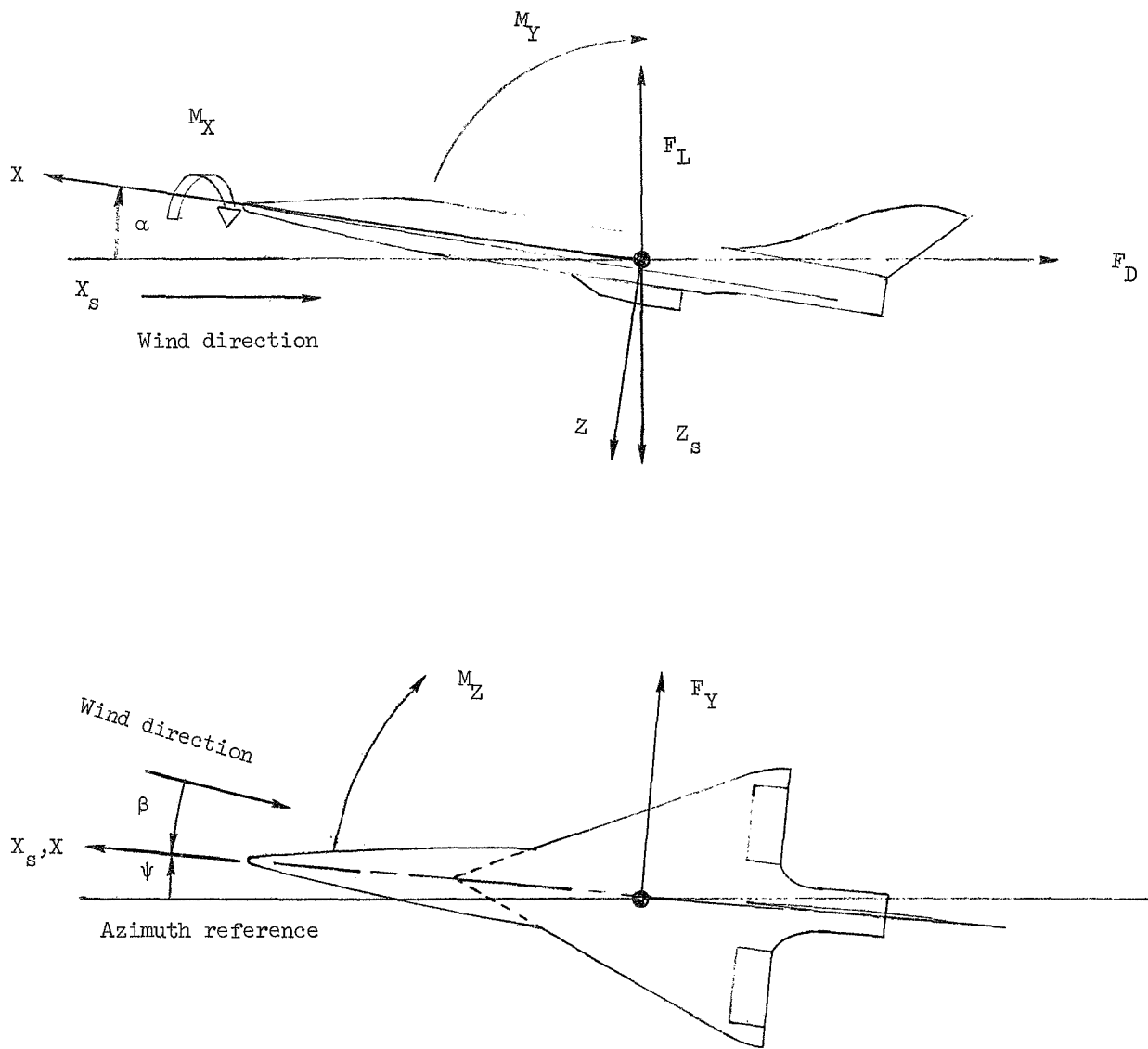
Figure 1.- System of axes used in investigation. Arrows indicate positive directions of moments, forces, and angles.

19.75
(50.1)

26.70
(67.8)

Station
63.38
(161.0)

24.38
(61.9)

13.40
(34.0)

Station A
17.38
(44.1)

65°

Station C
46.90
(119.1)

Station B
42.68
(108.4)

Station A

Station B

Station C

37.71
(95.8)

Moment Center
.51$\bar{c}$

65.88
(167.3)

Reference Dimensions
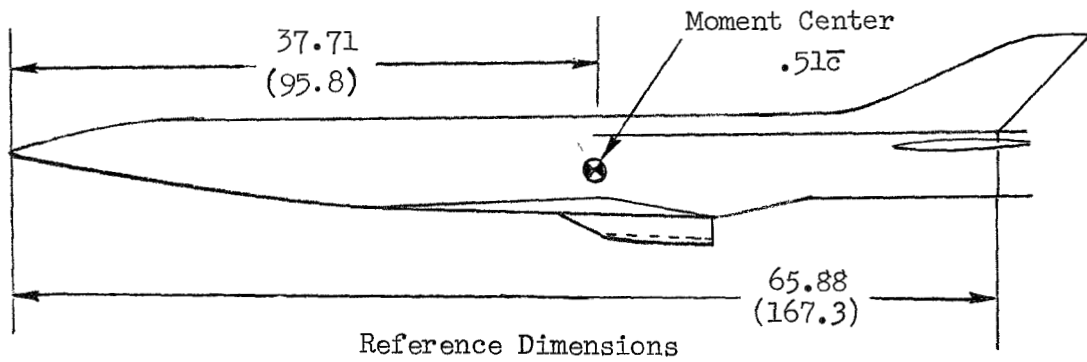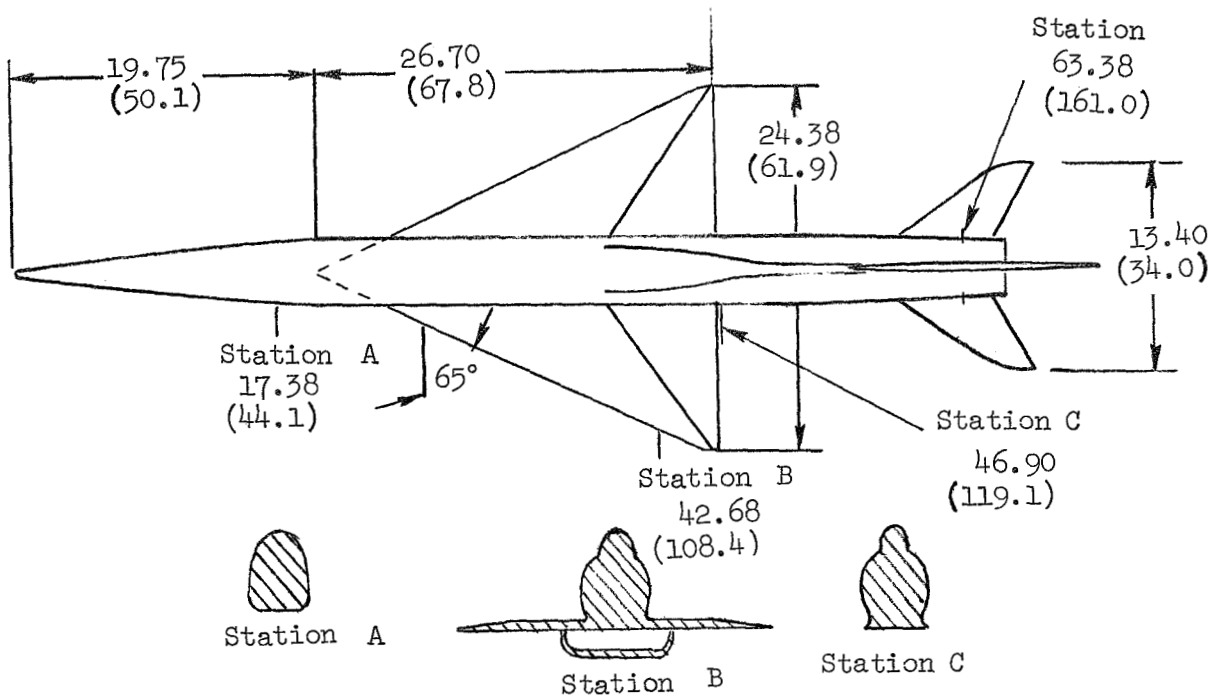
S   324 in.^{2} (2090.3 cm^2)

b   24.38 in. (61.9 cm)

$\bar{c}$ 17.88 in. (45.4 cm)

(a) Distinct wing-body configuration.

Figure 2.- Details of configurations used in investigation. Dimensions are given in inches (centimeters).
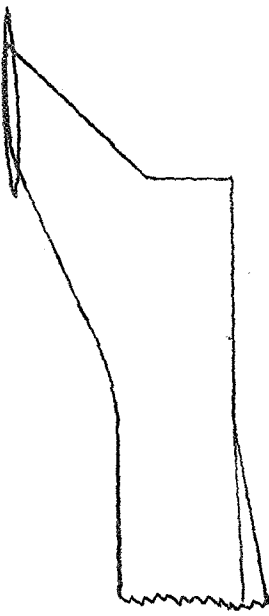
T-tail
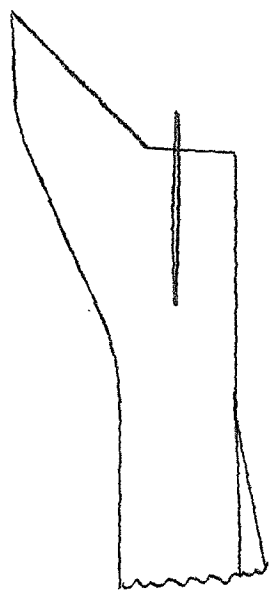
Original tail position
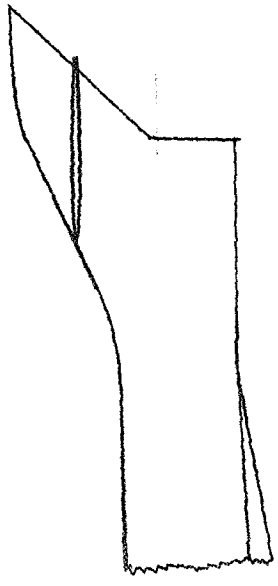
Midtail
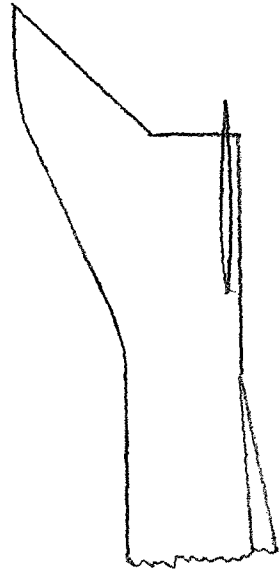
Low tail

(b) Vertical positions of horizontal tail tested with distinct wing-body configuration.

Figure 2.- Continued.

10
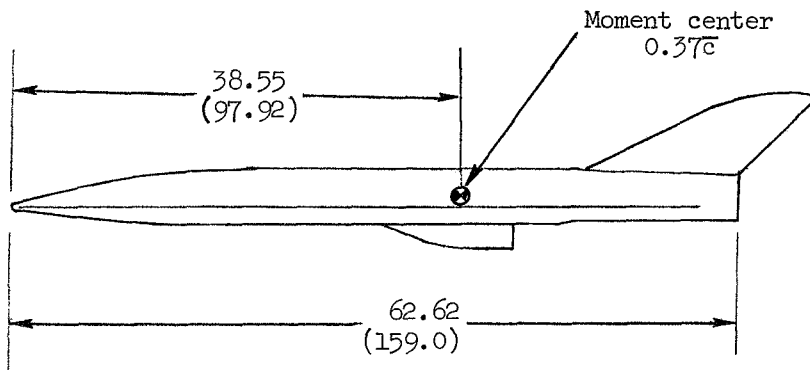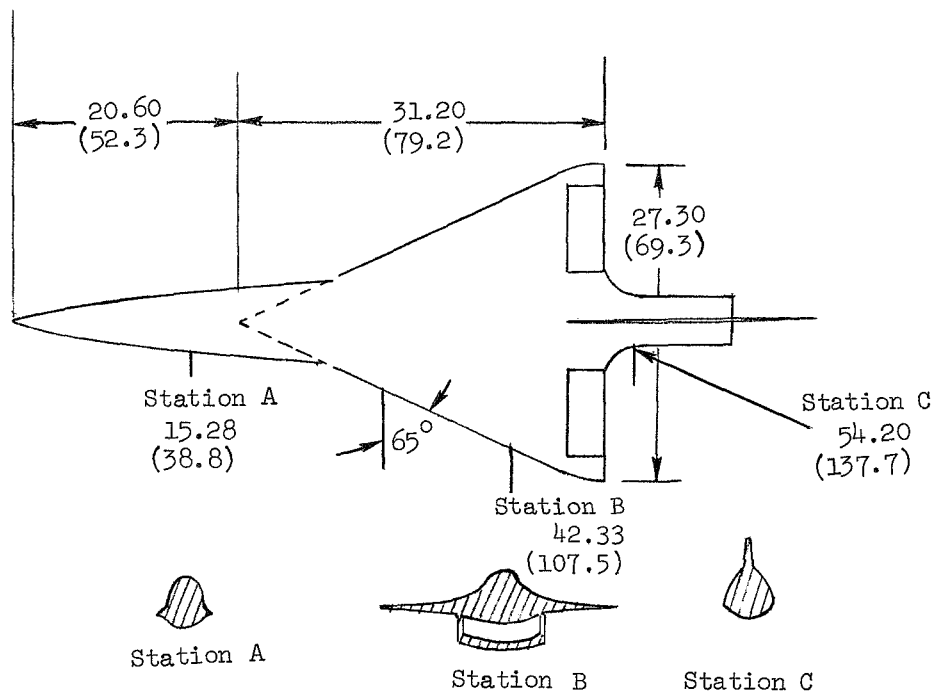
Reference Dimensions

S 453.2 in.^{2} (2923.9 cm^2)

b   27.30 in. (69.3 cm)

$\bar{c}$ 20.77 in. (52.8 cm)

(c) Blended wing-body configuration.

Figure 2.- Concluded.
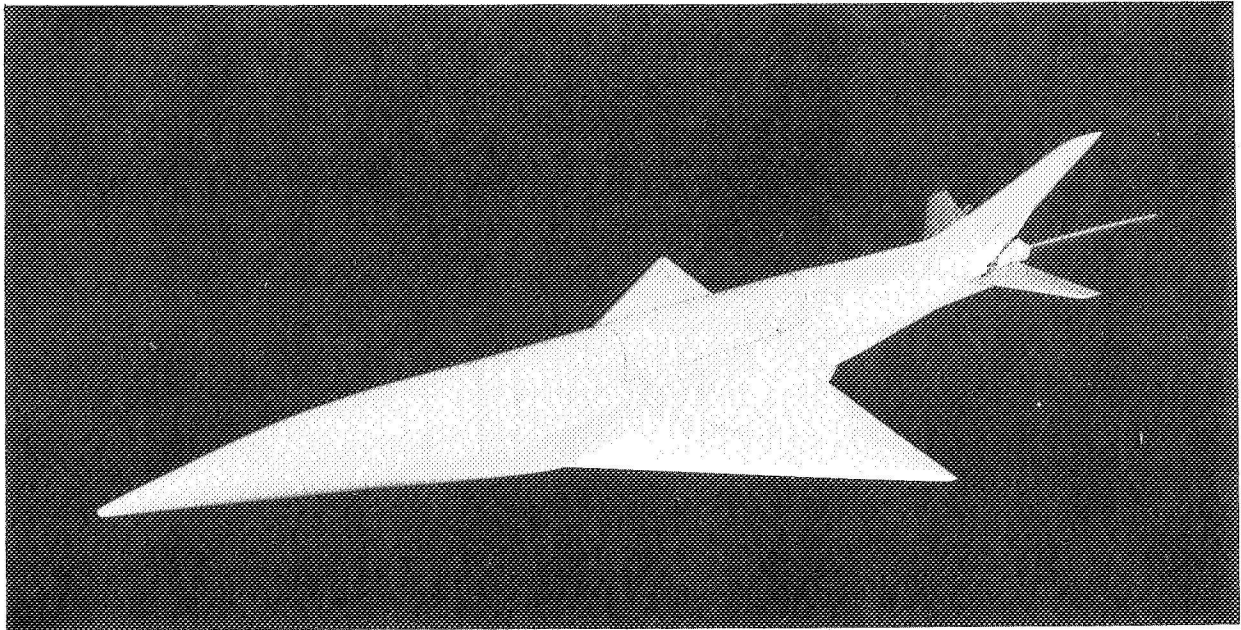
(a) Distinct wing-body configuration.   L-67-1301
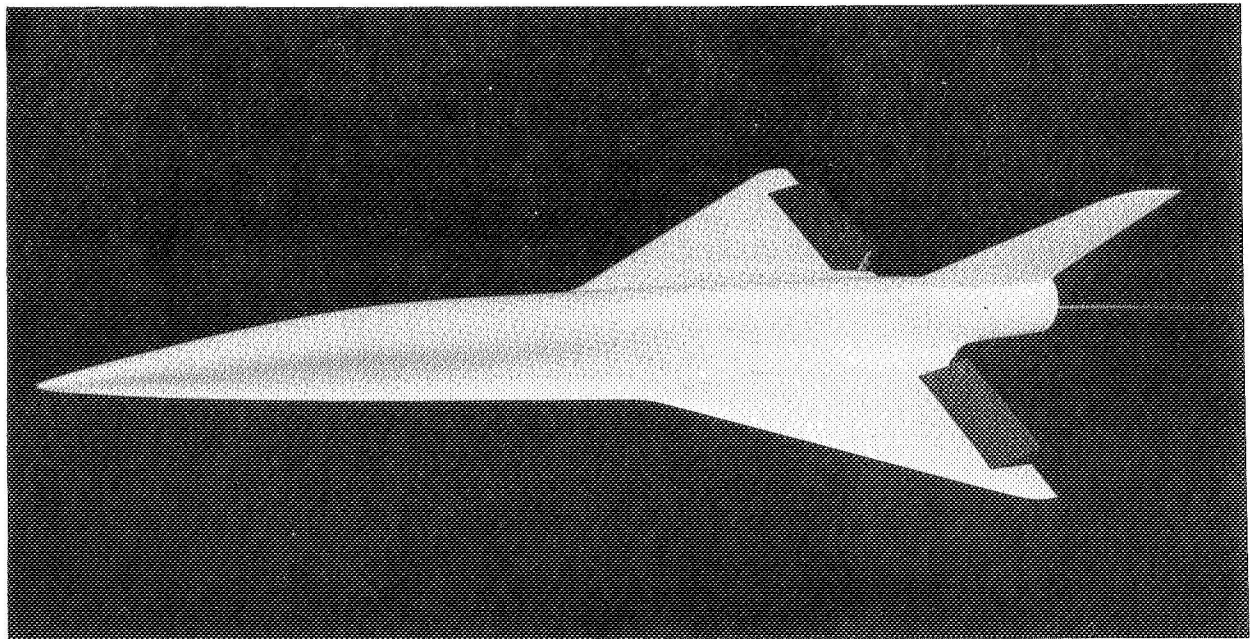
(b) Blended wing-body configuration.   L-67-1397

Figure 3.- Photographs of models used in investigation.
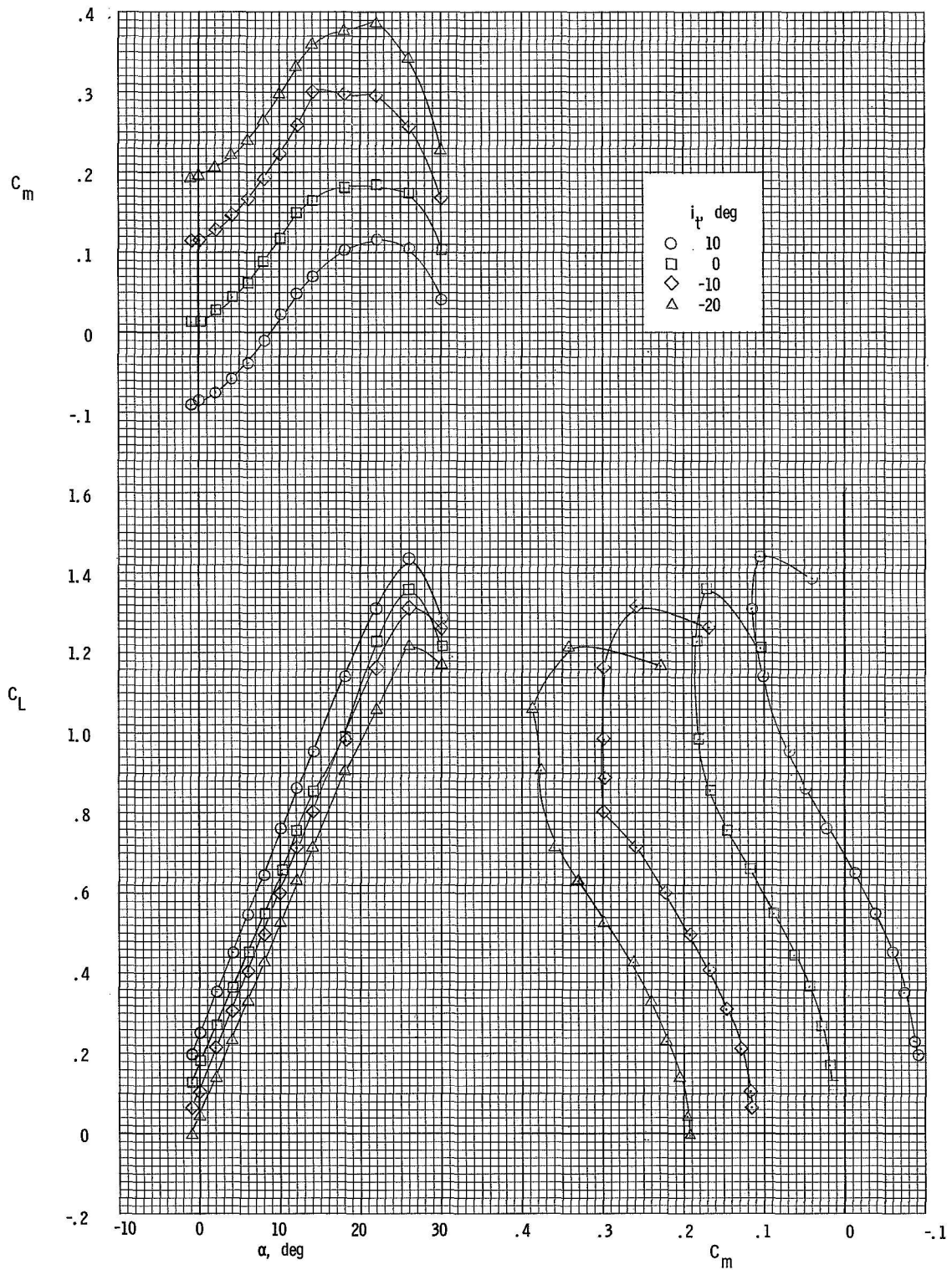
Figure 4.- Longitudinal characteristics of the distinct wing-body configuration. $\delta_{i,t} = 0°$; $\delta_r = 0°$.
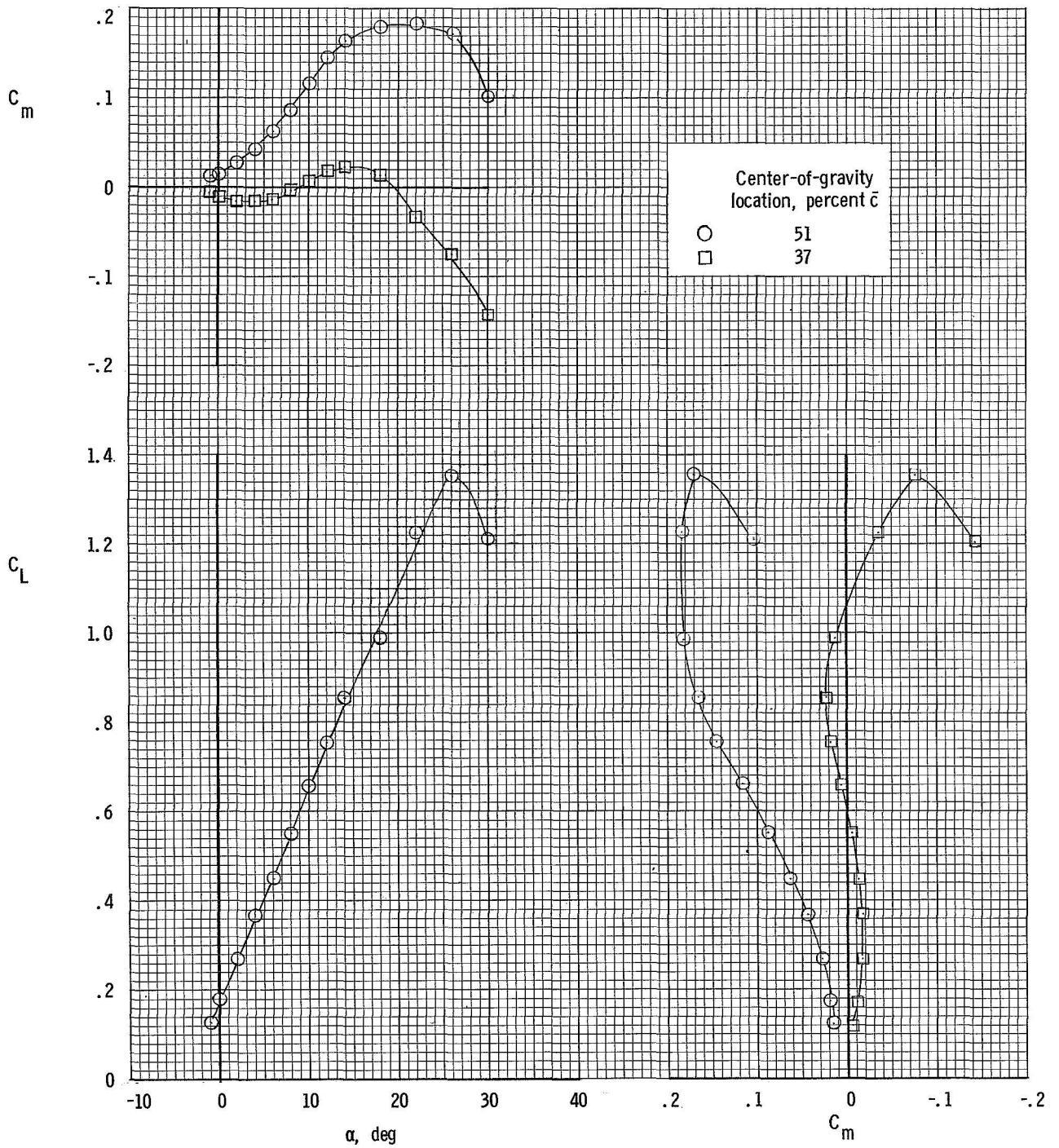
Figure 5.- Effect of center-of-gravity location on the static longitudinal characteristics of the distinct wing-body configuration. $i_t = 0^\circ$; $\delta_{i,t} = 0^\circ$; $\delta_r = 0^\circ$.
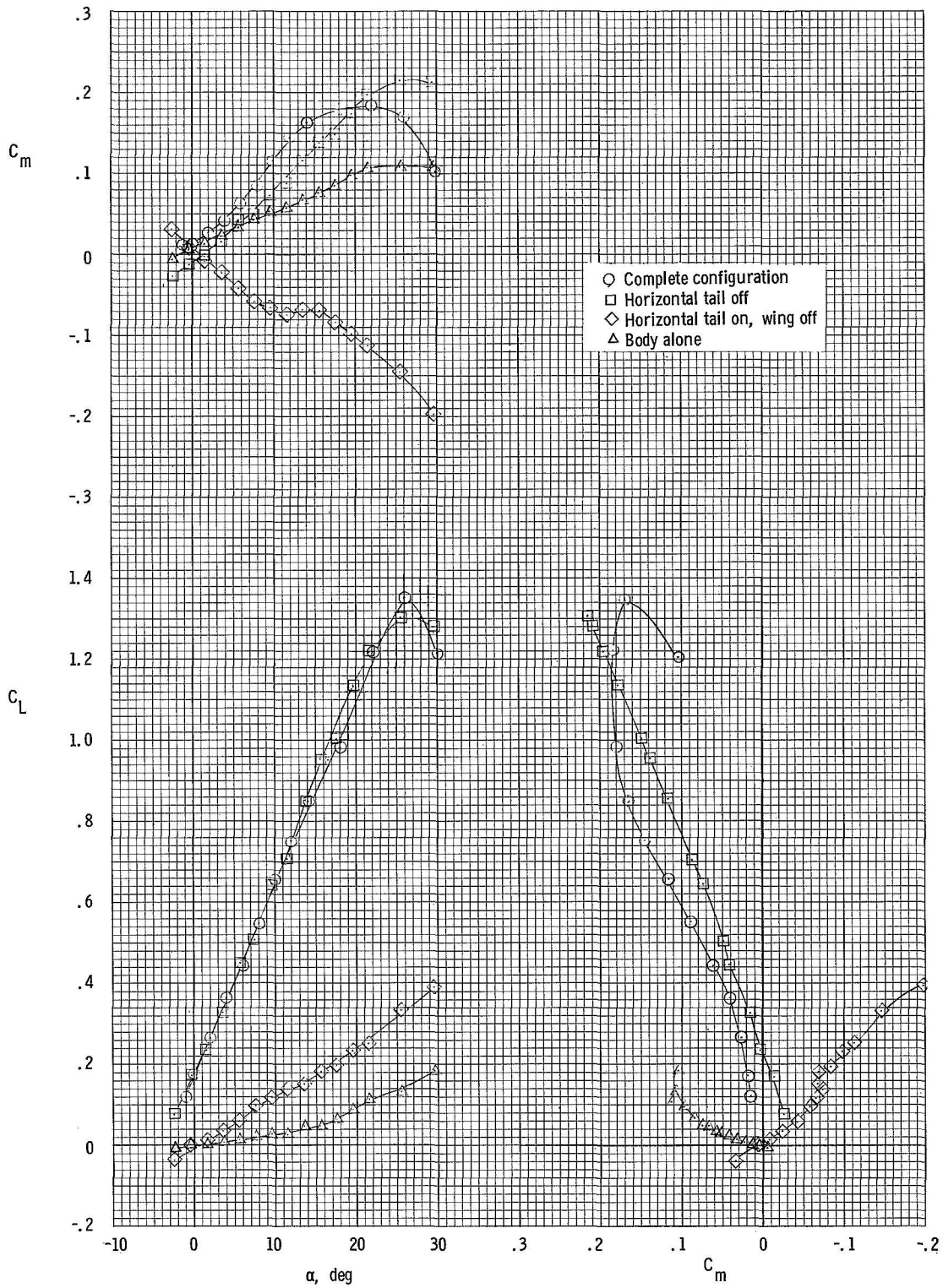
Figure 6.- Effect of various components on the longitudinal characteristics of the distinct wing-body configuration. $i_t = 0^0$; $\delta_{i,t} = 0^0$; $\delta_r = 0^0$.

15
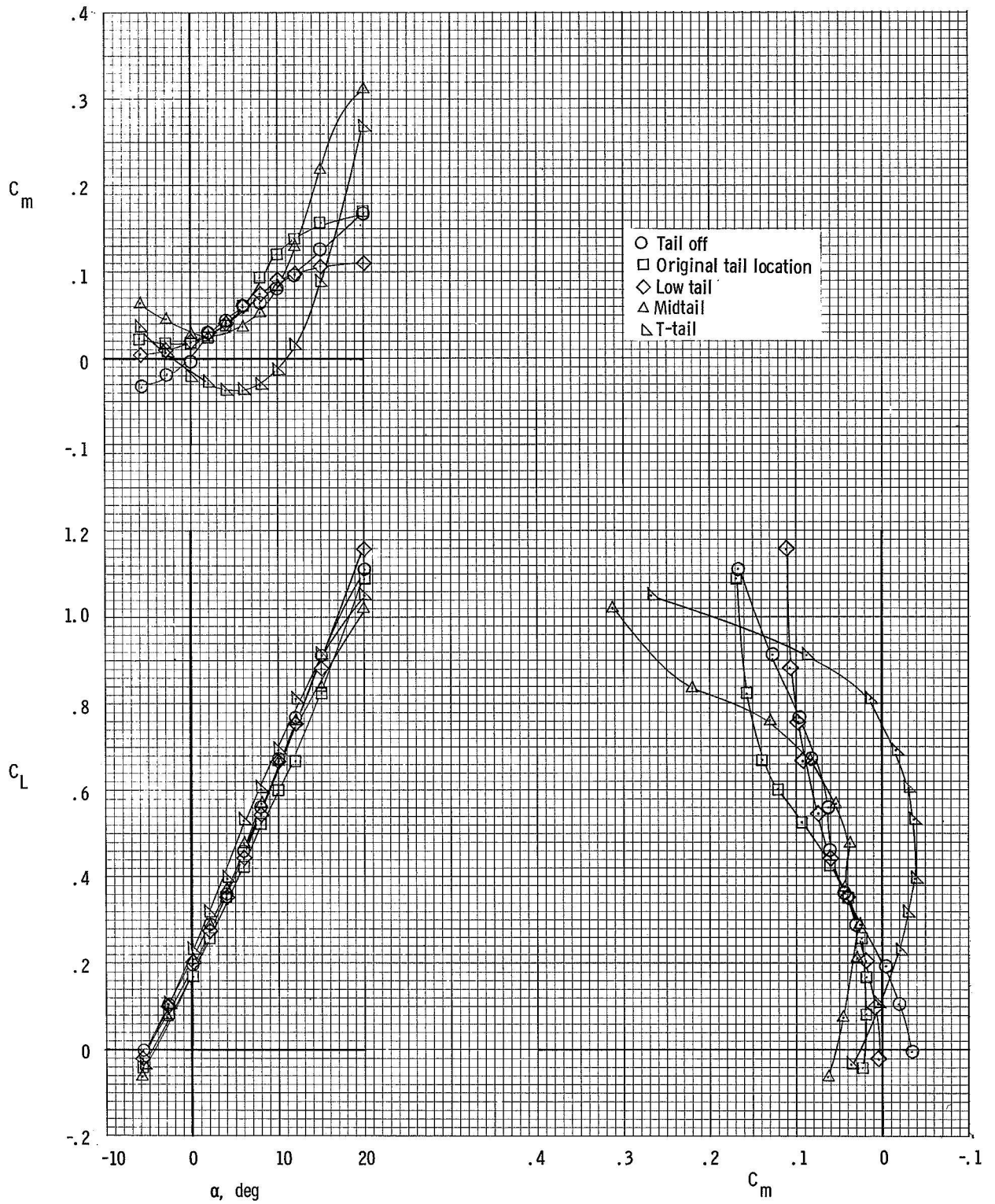
Figure 7.- Effect of vertical location of the horizontal tail on the longitudinal characteristics of the distinct wing-body configuration. $i_t = 0^0$; $\delta_{i,t} = 0^0$; $\delta_r = 0^0$.
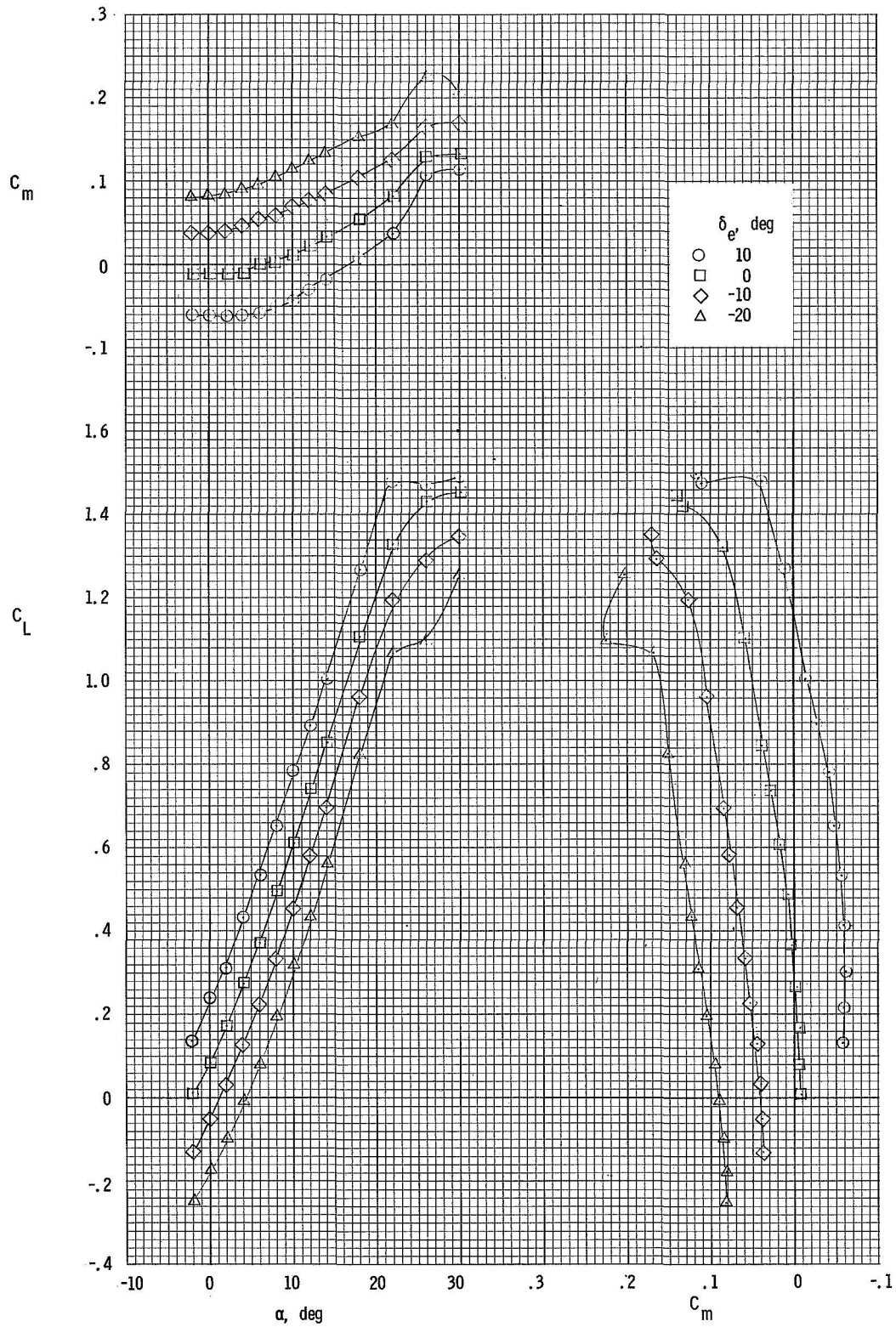
Figure 8.- Longitudinal characteristics of the blended wing-body configuration. $\delta_a = 0^0$; $\delta_r = 0^0$.
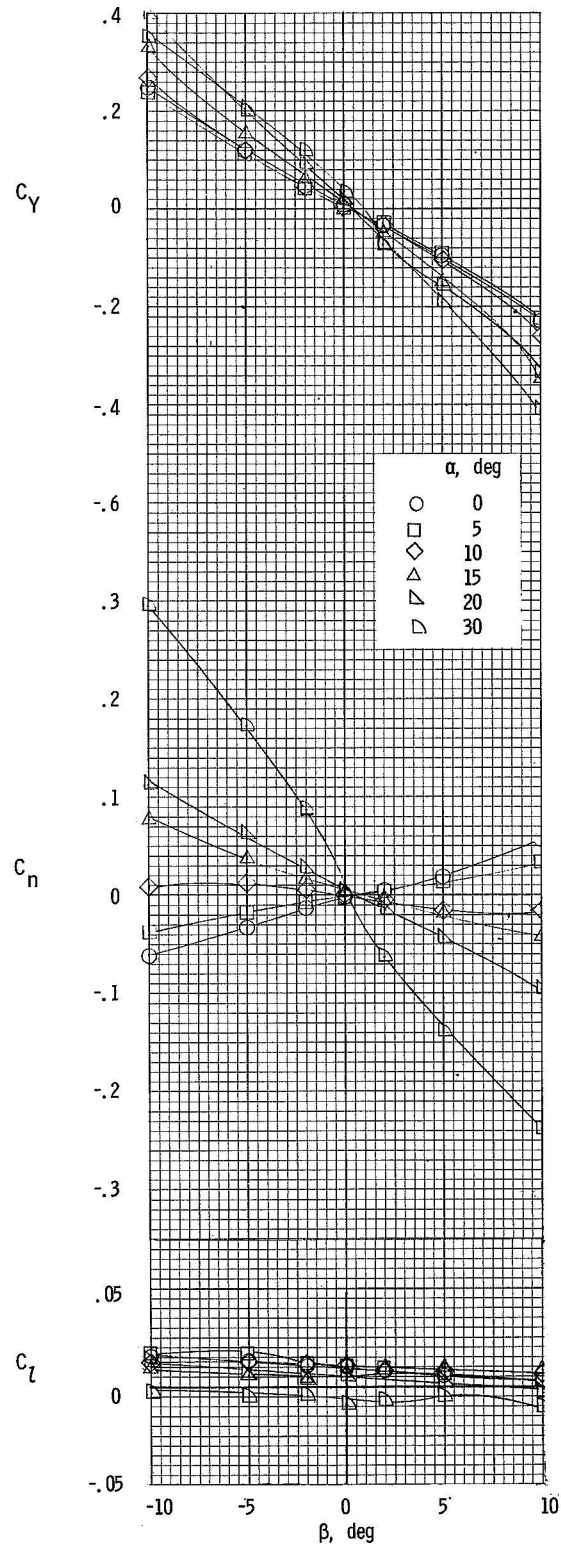
Figure 9.- Lateral characteristics of the distinct wing-body configuration. $i_t = 0^0$; $\delta_{i,t} = 0^0$; $\delta_r = 0^0$.

18
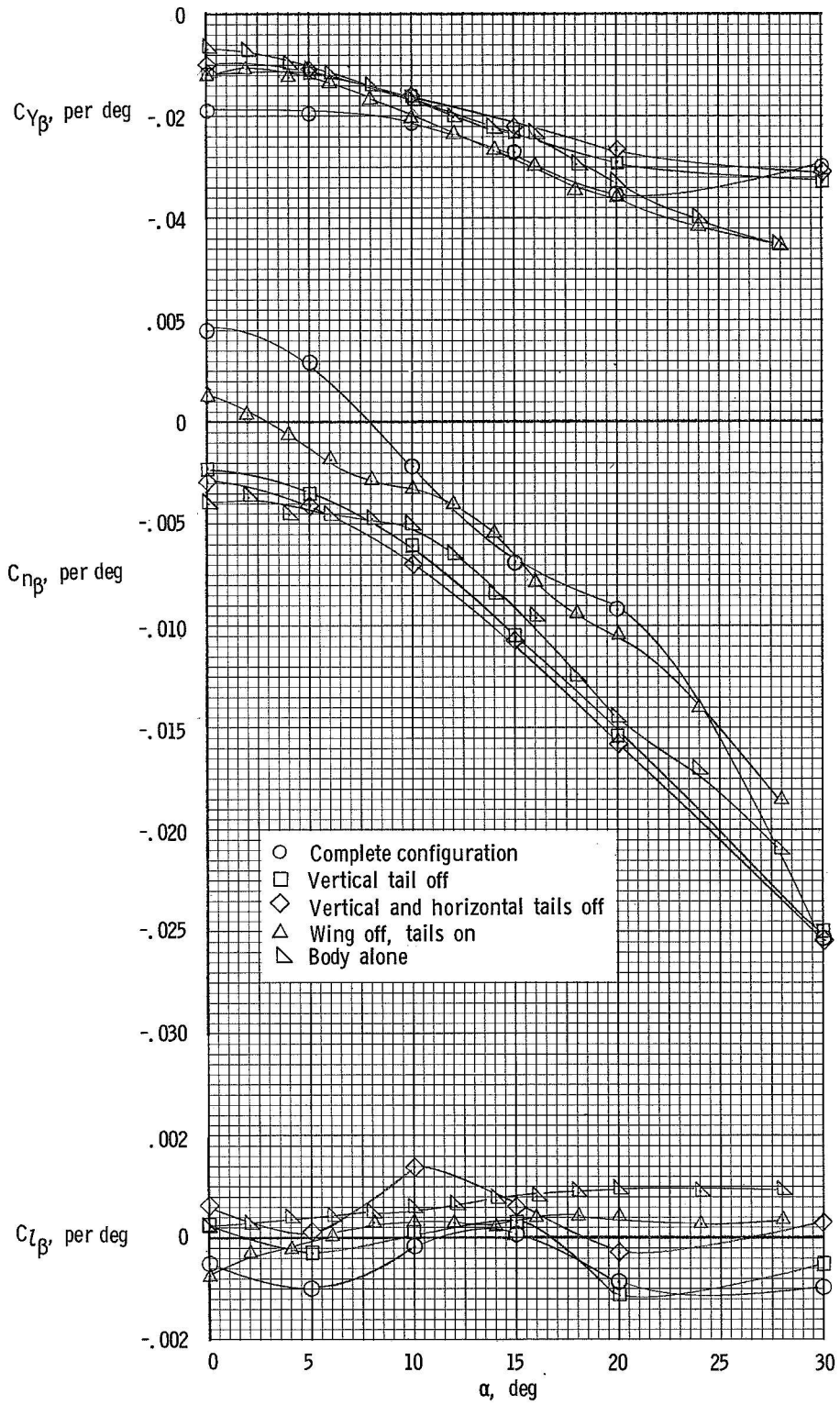
Figure 10.- Effect of various components on the lateral stability of the distinct wing-body configuration. $i_t = 0^o$; $\delta_{i,t} = 0^o$; $\delta_r = 0^o$.
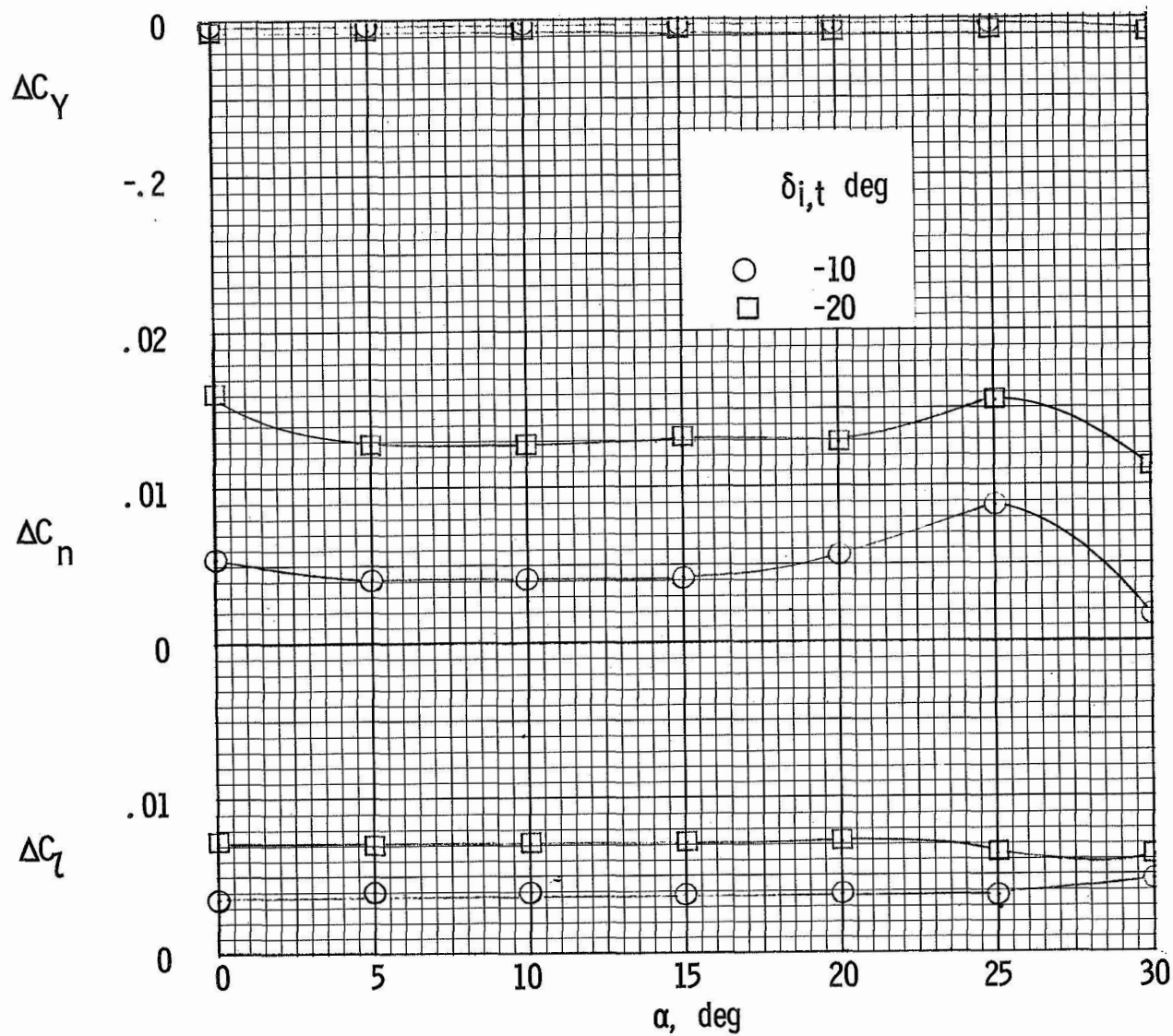
Figure 11.- Roll control effectiveness of the distinct wing-body configuration. $\delta_r = 0^o$; $\beta = 0^o$.
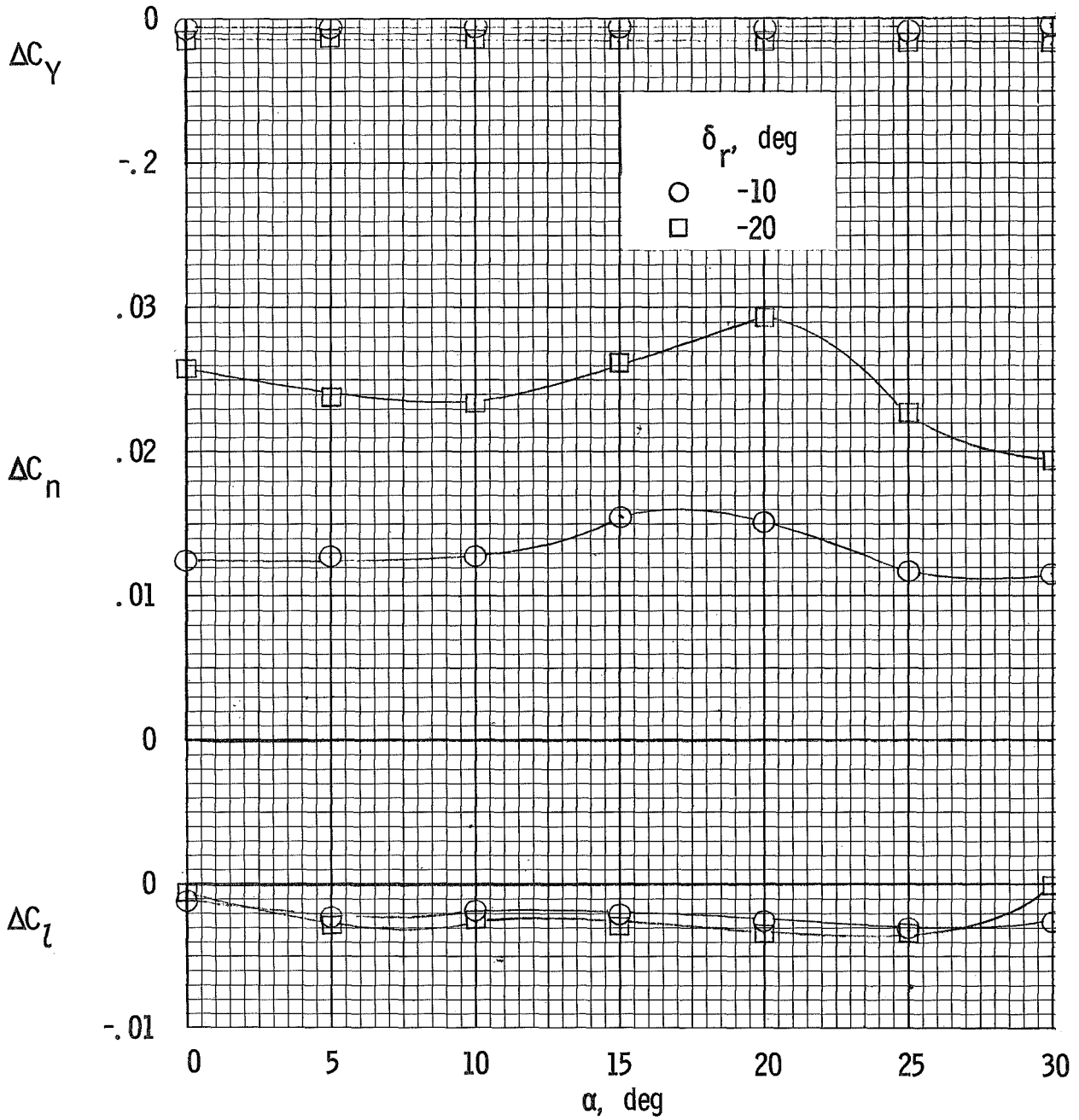
Figure 12.- Rudder control effectiveness of the distinct wing-body configuration. $\delta_{i,t} = 0^0$; $\beta = 0^0$.
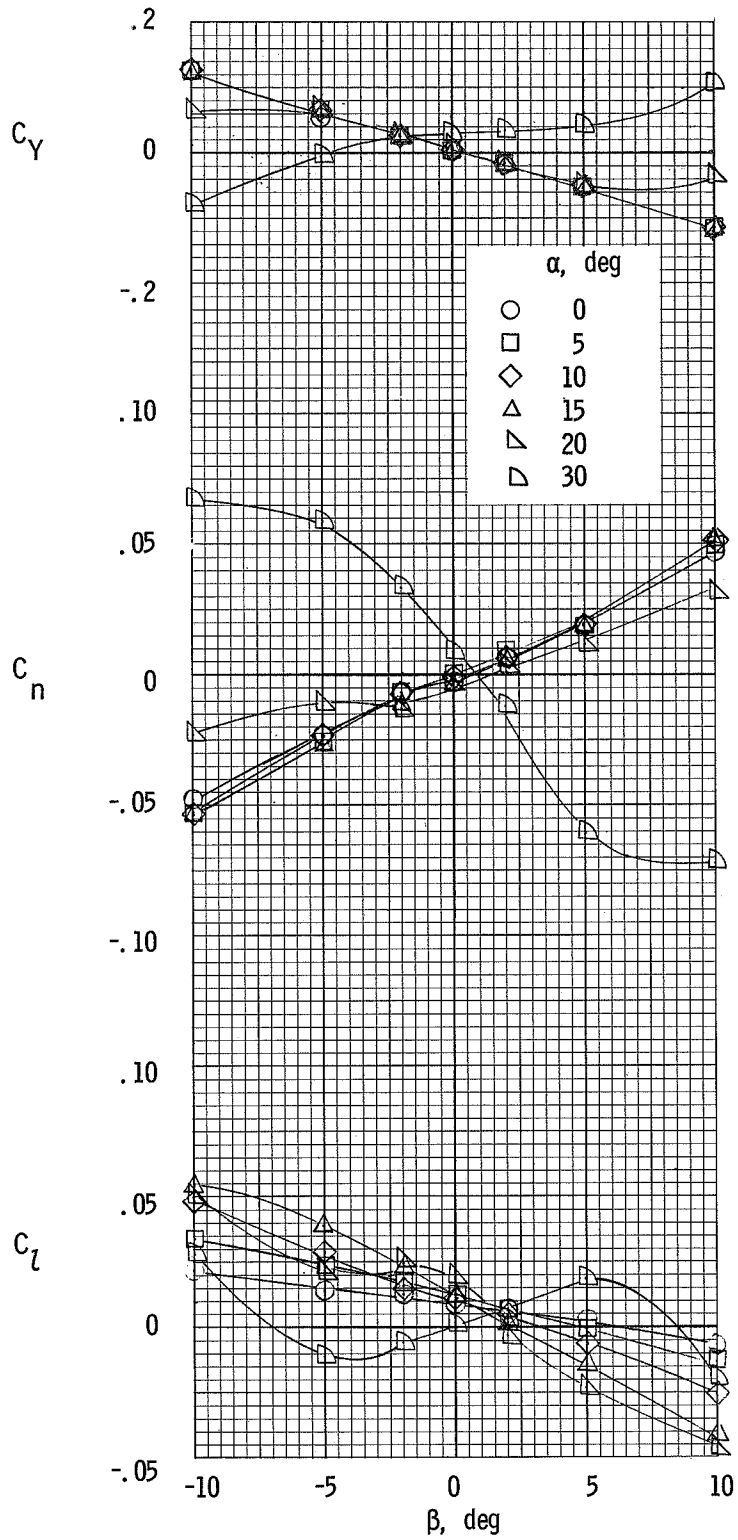
Figure 13.- Lateral characteristics of the blended wing-body configuration. $\delta_e = 0^0$; $\delta_a = 0^0$; $\delta_r = 0^0$.
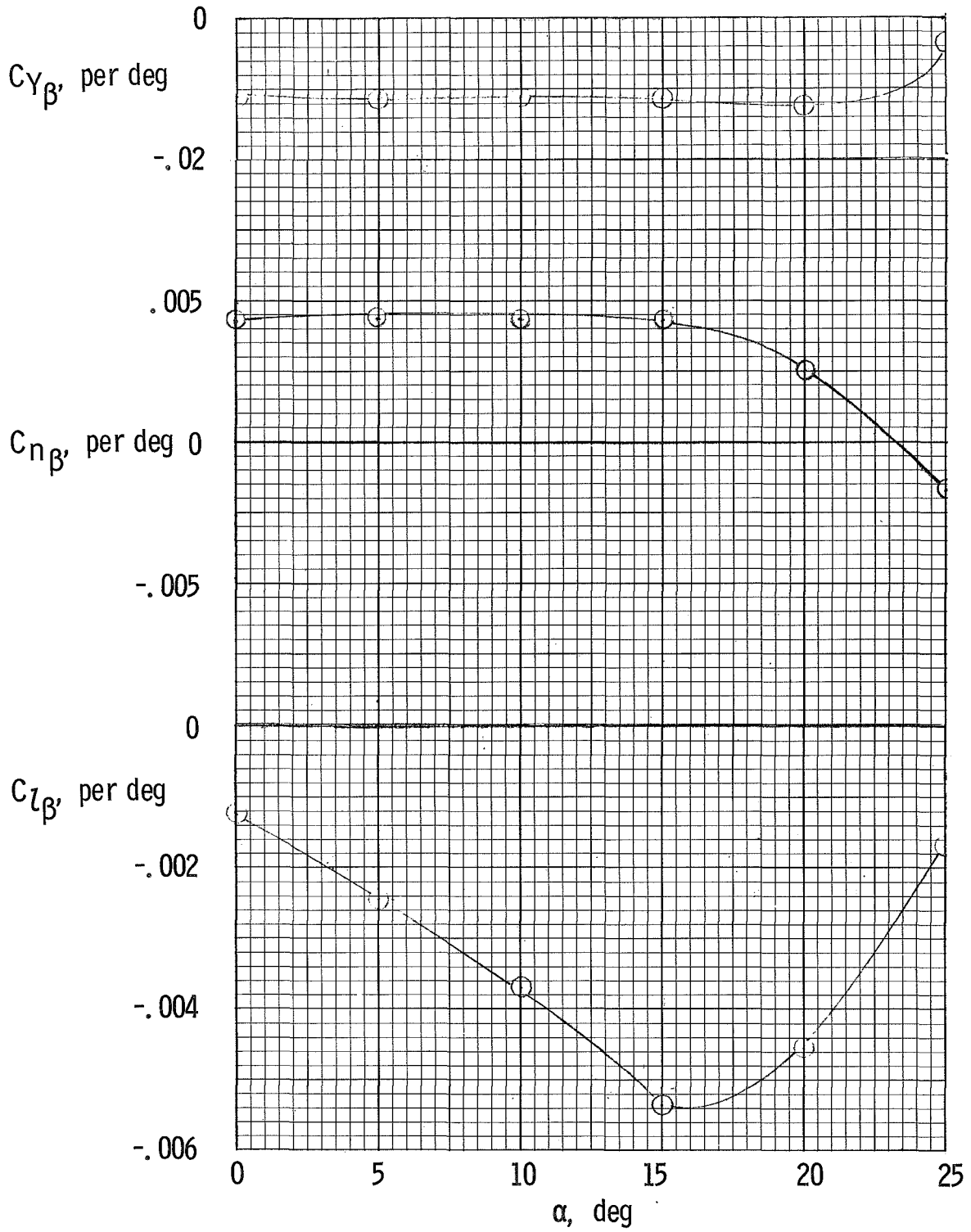
Figure 14.- Static lateral stability derivatives of the blended wing-body configuration. $\delta_e = 0°$; $\delta_a = 0°$; $\delta_r = 0°$.
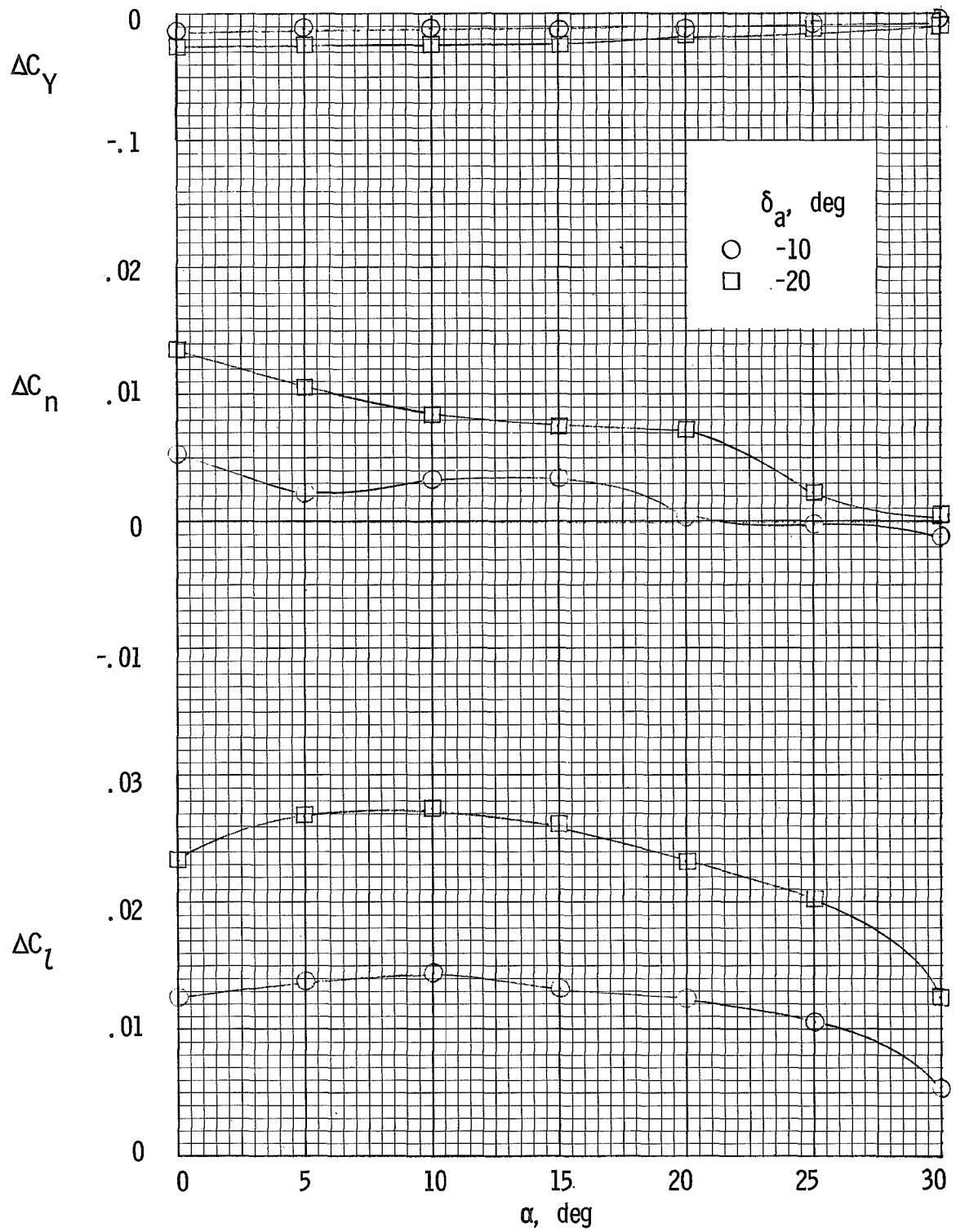
Figure 15.- Aileron control effectiveness of the blended wing-body configuration. $\delta_e = 0^o$; $\delta_r = 0^o$; $\beta = 0^o$.

24
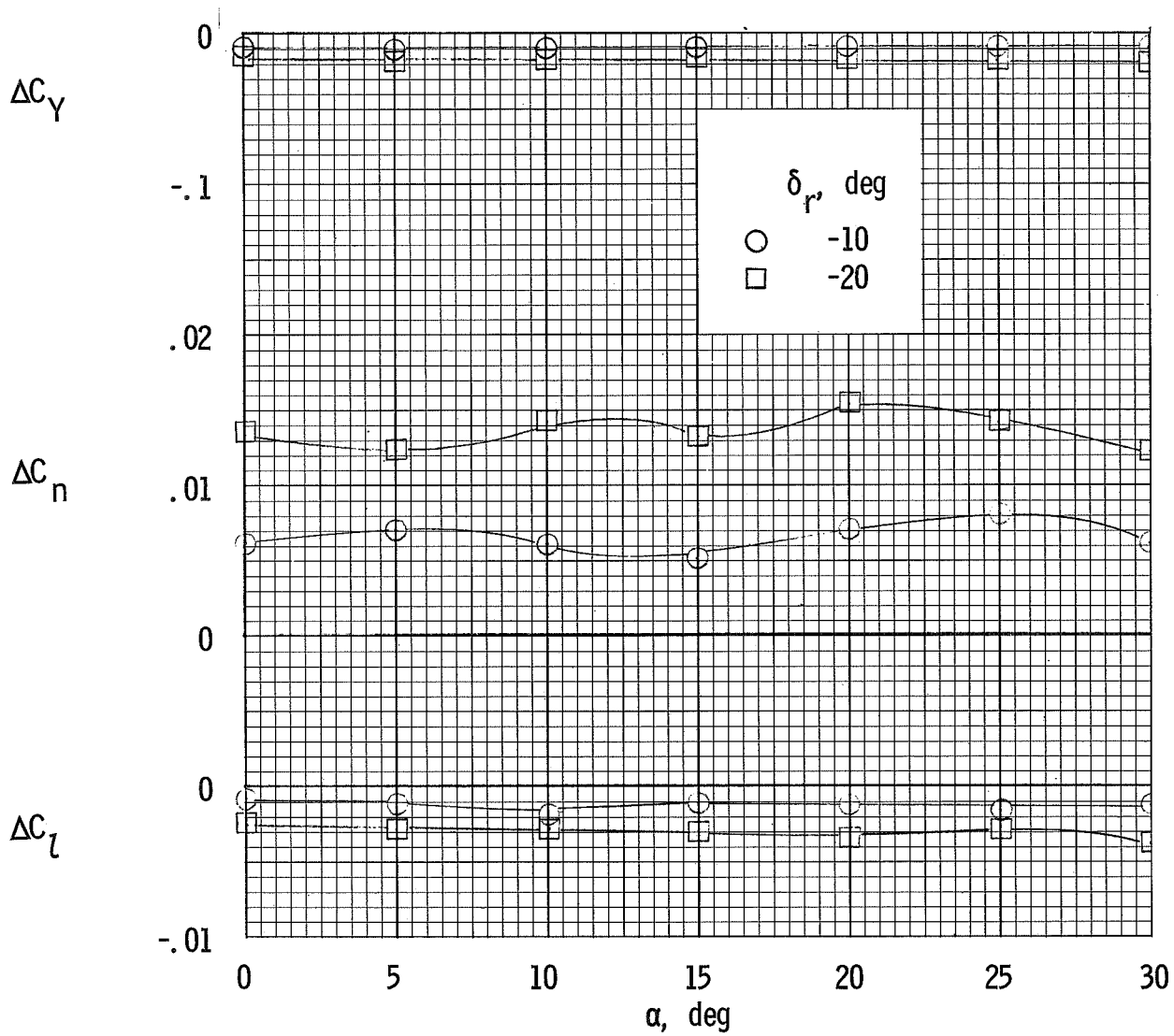
Figure 16.- Rudder control effectiveness of the blended wing-body configuration. $\delta_e = 0^0$; $\delta_a = 0^0$; $\beta = 0^0$.

"The aeronautical and space activities of the United States shall be conducted so as to contribute . . . to the expansion of human knowledge of phenomena in the atmosphere and space. The Administration shall provide for the widest practicable and appropriate dissemination of information concerning its activities and the results thereof."

— NATIONAL AERONAUTICS AND SPACE ACT OF 1958

NASA SCIENTIFIC AND TECHNICAL PUBLICATIONS

TECHNICAL REPORTS: Scientific and technical information considered important, complete, and a lasting contribution to existing knowledge.

TECHNICAL NOTES: Information less broad in scope but nevertheless of importance as a contribution to existing knowledge.

TECHNICAL MEMORANDUMS: Information receiving limited distribution because of preliminary data, security classification, or other reasons.

CONTRACTOR REPORTS: Scientific and technical information generated under a NASA contract or grant and considered an important contribution to existing knowledge.

TECHNICAL TRANSLATIONS: Information published in a foreign language considered to merit NASA distribution in English.

SPECIAL PUBLICATIONS: Information derived from or of value to NASA activities. Publications include conference proceedings, monographs, data compilations, handbooks, sourcebooks, and special bibliographies.

TECHNOLOGY UTILIZATION PUBLICATIONS: Information on technology used by NASA that may be of particular interest in commercial and other non-aerospace applications. Publications include Tech Briefs, Technology Utilization Reports and Notes, and Technology Surveys.

Details on the availability of these publications may be obtained from:

SCIENTIFIC AND TECHNICAL INFORMATION DIVISION

NATIONAL AERONAUTICS AND SPACE ADMINISTRATION

Washington, D.C. 20546